Spatially Concatenated Codes with Turbo Equalization for Correlated Sources

Khoirul Anwar, *Member, IEEE,* and Tad Matsumoto, *Fellow, IEEE*

***Abstract*—This paper proposes for single carrier signaling a simple structure that combines turbo equalization and decoding of correlated sources in multipath-rich multiuser Rayleigh fading multiple access channels (MAC), where the correlation between the sources is exploited by *vertical iterations* (*VI*) between the decoders. The bit-flipping model with a flipping probability p_e is used to express the correlation ρ between the sources as $\rho = 1 - 2p_e$. The proposed simple structure, spatially concatenated codes (SpCC), can achieve turbo-like performance over MAC channels suffering from severe inter-symbol interference (ISI), even though it uses short memory convolutional codes. First of all, to achieve turbo-like performance we introduce *VI*s to exploit the knowledge about the source correlation by exchanging extrinsic log-likelihood ratio (LLR) between the two decoders. We then add a rate-1 doped accumulator (D-ACC) to flexibly adapt for the variation of correlations between the sources. The results of computer simulations and extrinsic information transfer (EXIT) analysis confirm that in multipath-rich environments the proposed structure can achieve excellent performances, 1.02–1.28 dB away from the Slepian-Wolf-Shannon limit, at 1% outage probability for $0 < \rho \leq 1$.**

***Index Terms*—Source correlation; Turbo equalization; Slepian-Wolf coding; Convolutional codes;**

I. Introduction

ONE of the most important issues in multi-node communications is the existence of the correlation in information transmitted from the multiple sources. The correlation can be utilized to reduce the energy consumption [1] for reliable data transmission from multiple sources to a common receiver. Turbo equalization [2], originally proposed to reduce the complexity of super-trellis based *maximum a posteriori* (MAP) equalizer in multipath-rich wireless communications by utilizing the turbo concept, can be applied for the communication systems with correlated sources. A goal of this paper is to propose a technique that can make efficient use of the source correlation with the aim of its applications to, for example, video surveillance or sensor networks.

Despite the volume of publications describing space-time transmission techniques for *independent* multiple sources, to the authors' best knowledge, only a few have been known for turbo equalization with the *correlated* sources over broadband wireless channel suffering from severe inter-symbol interference (ISI). In [3], turbo equalization has been applied for hidden Markov model (HMM)-based correlated sources over an ISI channel assuming that side information is available at the decoder. The technique is extended to the case where users transmits their correlated source information simultaneously over the channel exhibiting frequency selectivity [4]. Ref. [4] uses a joint detection and state estimation technique according to the maximum *a posteriori* probability (MAP) criterion to jointly equalize and estimate the correlated sources corrupted by the Hidden Markov error source, by using a sum-product algorithm. However, since no optimality consideration is provided in [4], this technique achieves still quite far away in performance, roughly 3.2 – 9.0 dB from the Slepian-Wolf-Shannon (SW-Shannon) limit.

A constructive "super" code using Turbo code as its constituent code, called as super Turbo codes (SuTC), is proposed in [5] with the aim of achieving the SW-Shannon capacity limit in additive white Gaussian noise (AWGN) channel. Unfortunately, when SuTC is extended to Rayleigh fading multiple access channel (MAC), the performance is not satisfactory [6] which motivates the authors of [6] to use low-density generator matrix (LDGM) codes. The LDGM codes is effective when the correlation is high, however, places relatively high error floor when the correlation is low. Hence, the challenge has been to construct a simple structure that: (1) approaches closer to the SW-Shannon limit performance, (2) is applicable for a wide range of correlations, and (3) lowers the error floor.

The SW coding theorem, introduced by Slepian and Wolf in 1973 [7], has drawn much attention recently with the aim of its applications to a variety of systems such as sensor networks [8], robust video transmission for wireless multimedia applications [9], and compression of encrypted data [10]. Furthermore, SW coding has recently been applied to relay and cooperative network systems [11].

The SW coding theorem constitutes a region of achievable rates $\mathcal{R}_1$ and $\mathcal{R}_2$ when considering the lossless compression of two correlated sources b_1 and b_2 sending data to a common *joint* decoder. The region is an unbounded polygon with two corner points, where b_1 is compressed at its entropy $\mathcal{H}(b_1)$ while b_2 can be compressed at a smaller rate than its entropy $\mathcal{H}(b_2)$, but larger than their conditional entropy $\mathcal{H}(b_2|b_1)$ or vice versa. The SW bound is given by the three inequalities,

$$\mathcal{R}_1 \geq \mathcal{H}(b_1|b_2), \tag{1}$$

$$\mathcal{R}_2 \geq \mathcal{H}(b_2|b_1), \tag{2}$$

$$\mathcal{R}_1 + \mathcal{R}_2 \geq \mathcal{H}(b_1, b_2), \tag{3}$$

where $\mathcal{H}(b_1, b_2)$ is the joint entropy. The contribution of the SW coding theorem is the discovery that the compression can be performed even if both sources do not communicate with each other as long as the joint decoder is able to know or estimate the source correlation.

In the wireless multiuser communication system exemplified by the block diagram in Fig. 1, the turbo iterations are performed independently for the each user [12]. This iteration is referred to as *horizontal iteration* (*HI*) in this paper. However, if the both users transmit identical source information using different interleavers, we found [13] that *vertical iterations* (*VI*) between the decoders can transform two independent convolutional codes into a Turbo-like code, which yields significant performance gain.

In this paper, based on our previous work in [13], we propose for single carrier signaling a simple structure, spatially concatenated code for SW systems (SpCC-SW), for wireless communications over multipath Rayleigh fading MAC, where joint turbo equalization and decoding with the *HI* and *VI*, are performed. The receiver

K. Anwar is with the School of Information Science, Japan Advanced Institute of Science and Technology (JAIST), 1-1 Asahidai, Nomi, Ishikawa, JAPAN 923-1292, e-mail: anwar-k@jaist.ac.jp.

T. Matsumoto is with the School of Information Science, Japan Advanced Institute of Science and Technology, Hokuriku, JAPAN 923-1292, e-mail: matumoto@jaist.ac.jp and Center for Wireless Communication, University of Oulu, FI-90014 Finland. email: tadashi.matsumoto@ee.oulu.fi.

This research is supported in part by the Japan Society for the Promotion of Science (JSPS) Grant under Scientific Research Kiban (C) No. 22560367 and (B) No. 23360170.

Manuscript received month dd, 2011; revised month dd, 2011.

utilizes multiple antennas, of which outputs are followed by the latest version of the turbo equalization, frequency-domain soft cancellation and minimum mean squared error (FD/SC-MMSE) filtering, as an efficient equalization technique[1] in this paper.

First of all, we revisit our technique presented in [13], which introduces *VI*, and show that it can be regarded as a special case of the SW system with fully correlated sources. Each transmitter has one antenna and its own encoder, separated by an interleaver but they have a common source. At the receiver side, two iterative processes, *HI* and *VI*, are invoked. The *HI* performs turbo equalization with the aim of combining energies of all the multi-path components and achieving path diversity gain,[2] while eliminating the interference components from other antennas or inter-antenna interference (IAI). The *VI* is used to further enhance the performance, aiming at achieving coding gain on the top of the diversity gain.

From the viewpoint of the SW coding, the *VI* is a process of exploiting the correlation knowledge between the two sources. On the other hand, from the viewpoint of channel coding, the *VI* loop structure is exactly the same as turbo loop in the parallel concatenated turbo decoder. The only difference is that in parallel concatenated Turbo codes, the encoded sequence is multiplexed in the time domain, while in the proposed SpCC-SW case, the multiplexing is in the spatial domain.

We utilize a random bit-flipping correlated sources model with bit-flipping probability p_e between the two sources, b_1 and b_2, as in [5]. At the receiver, the extrinsic log-likelihood ratio (LLR) is updated due to the bit-flipping probability p_e, every time the *VI* loop is activated, as discussed in the Section II-B.

To maximize the benefit of exploiting the knowledge about correlation by the *VI*, we apply a rate-1 doped accumulator (D-ACC) to reduce the error floor. The use of D-ACC further invokes the idea that two relatively short memory convolutional codes is better suited for the proposed structure, because whether or not the iterative detection and decoding system can achieve good performance is not a matter of the code *strength*, but the matter of the matching of the extrinsic information transfer (EXIT) characteristics. We conducted via intensive EXIT chart analyzes as a preliminary work of this paper. In this paper, it is shown that the proposed SpCC-SW with relatively short memory convolutional constituent codes can achieve better performances in terms of bit-error-rate (BER) performances compared with SuTC in [5].

II. Proposed Spatially Concatenated Codes based on Slepian-Wolf System

In this section, we propose SpCC-SW structure, of which receiver is composed of a common turbo equalizer and two short memory convolutional decoders. The proposed SpCC-SW structure is shown in Fig. 2.

A. Transceiver Structure

The transmitter has three interleavers, Π_0, Π_1, Π_2, with two encoders as shown in Fig. 2. The bitstream b_2 is a Π_0-interleaved version of b_1 where some of the bits are "flipped" as detailed in Subsection II-B. The interleavers Π_0 is introduced to exploit the correlation knowledge via the *VI*. The Interleavers, Π_1 and Π_2, interleave the coded bits x and y, coded by encoders C_1 and C_2, respectively, to obtain the interleaved sequences x' and y', and hence are longer than Π_0. Finally, D-ACC on each branch provides doped-accumulated bit sequences x'' and y''. They are BPSK-modulated to form a symbol vector $\mathbf{s} = [\mathbf{s}_1, \mathbf{s}_2]^T$, and then cyclic prefix (CP) is appended at the head of each block. The symbol vectors are finally transmitted from the antenna 1 and 2, Tx_1 and Tx_2, respectively.[3]

After the removal of CP, a block-wise expression of the received signal $\mathbf{r}$, received via a multipath block Rayleigh fading channel, is expressed using circulant matrix $\mathbf{H}_c$ as

$$\mathbf{r} = \mathbf{H}_c\mathbf{s} + \mathbf{n} \in \mathbb{C}^{2K\times 1}, \tag{4}$$

where $\mathbf{n}$ is a zero mean complex additive white Gaussian noise vector with its covariance $\mathbb{E}[\mathbf{n}\mathbf{n}^H] = \sigma^2$, and $\sigma^2 = 10^{-\Gamma[\mathrm{dB}]/10}$. $\sigma^2/2$ is the noise variance per dimension and $\Gamma = \mathbb{E}[\gamma]$ is the average signal-to-noise power ratio (SNR), with γ being the instantaneous SNR. We assume that the average SNRs at receive antenna 1 (Rx_1) and receive antenna 2 (Rx_2), Γ_1 and Γ_2 , respectively, are equal, i.e., $\Gamma_1 = \Gamma_2 = \Gamma$.

B. LLR Update for Bit-flipping Correlated Sources Model

A simple bit flipping model is used to parameterize the correlation between the sources b_1 and b_2 as in [5]. The binary source sequence b_1 is denoted as $b_1 = [b_1^1, b_1^2, \cdots, b_1^k, \cdots b_1^K]$, and the source of b_2 as $b_2 = [b_2^1, b_2^2, \cdots, b_2^k, \cdots b_2^K]$, where K is the information block length. We assume that the sequence b_1 satisfies the i.i.d condition with $\Pr(b_1^k = 0) = 0.5$, $\Pr(b_1^k = 1) = 0.5$. Then, the sequence b_2 is defined as

$$b_2^k = b_1^k \oplus e^k, \tag{5}$$

where $\oplus$ indicates a modulo 2 addition and $e^k \in \{0, 1\}$ is the random variable for the k-th source bit with probabilities $\Pr(e^k = 1) = p_e$ and $\Pr(e^k = 0) = 1 - p_e$, which is independent of b_1^k. The conditional probability is then given by

$$\Pr(b_2^k = 0|b_1^k = 1) = \Pr(b_2^k = 1|b_1^k = 0) = p_e, \tag{6}$$

$$\text{and } \Pr(b_2^k = 0|b_1^k = 0) = \Pr(b_2^k = 1|b_1^k = 1) = 1 - p_e, \tag{7}$$

where parameter p_e has a value range of $0 \leqslant p_e \leqslant 0.5$. The correlation between the two sources is then expressed as

$$\rho = 1 - 2p_e. \tag{8}$$

With the source model described above, the sequences of the binary random variables b_1^k and b_2^k in source b_1 and b_2, respectively, are still i.i.d in terms of the bit index k (not correlated in time) and the appearances of 0 and 1 are equiprobable. Therefore, the corresponding entropy $\mathcal{H}(b_1) = \mathcal{H}(b_2) = 1$. On the other hand, by assuming that K is large enough[4], the conditional entropy $\mathcal{H}(b_1|b_2)$ is given by

$$\mathcal{H}(b_1|b_2) = \lim_{K\to\infty} \frac{1}{K}\mathcal{H}(b_2^1, \cdots, b_2^K|b_1^1, \cdots, b_1^K) = \mathcal{H}(p_e), \tag{9}$$

where $\mathcal{H}(p_e) = -p_e \log_2(p_e) - (1 - p_e)\log_2(1 - p_e)$ is a binary entropy of random sequence e. The achievable SW region $(\mathcal{R}_1, \mathcal{R}_2)$ with this model is

$$\mathcal{R}_1 \geq \mathcal{H}(p_e), \tag{10}$$

$$\mathcal{R}_2 \geq \mathcal{H}(p_e), \tag{11}$$

$$\text{and } \mathcal{R}_1 + \mathcal{R}_2 \geq 1 + \mathcal{H}(p_e). \tag{12}$$

[1] It should be noted here that the concept of SpCC-SW system is independent of the equalization schemes, e.g., MAP equalizer [4] that can achieve obviously better performance than FD/SC-MMSE, but authors in [3] shows that in the presence of source correlation, the performance difference is minor.

[2] Since the receiver uses two antennas, *HI* also achieves the space diversity. However, in multipath-rich environment the path diversity is a dominant factor of the performance improvement.

[3] A delay of τ is added to compensate the additional interleaver Π_0 between the sources b_1 and b_2.

[4] In the simulations, we consider $K = 2,560$ bits which is long enough to satisfy the conditional entropy definition.

Due to the correlation between the sources, the extrinsic LLR of the uncoded information bits, obtained as a result of the Bahl-Cocke-Jelinek-Raviv (BCJR) algorithm [14], has to be modified in the *VI*. As in [5], we use the following probability update for b_2:

$$\begin{aligned} \Pr(b_2=0) &= (1-p_e)\Pr(b_1=0)+p_e\Pr(b_1=1) \\ \text{and } \Pr(b_2=1) &= (1-p_e)\Pr(b_1=1)+p_e\Pr(b_1=0), \end{aligned} \quad (13)$$

where the symbol timing index k has been deleted for simplicity, and so is the case later on. The probability update for b_1 is performed in the same way as (13).

The LLR updating function $f_c(\cdot)$ corresponding to (13) for b_1 is

$$\begin{aligned} L^{b_1}_{e,D_1,updated} &= \ln \frac{(1-p_e)e^{L^{b_1}_{e,D_1}}+p_e}{(1-p_e)+p_e e^{L^{b_1}_{e,D_1}}}, \\ &= \ln \frac{(1-\rho)+(1+\rho)e^{L^{b_1}_{e,D_1}}}{(1+\rho)+(1-\rho)e^{L^{b_1}_{e,D_1}}} \\ &= f_c(\rho, L^{b_1}_{e,D_1}) \end{aligned} \quad (14)$$

where $L^{b_1}_{e,D_1}$ is the extrinsic LLRs of b_1. Similarly, the updated extrinsic LLR $L^{b_2}_{e,D_2}$ for b_2 is $L^{b_2}_{e,D_2,updated} = f_c(\rho, L^{b_2}_{e,D_2})$.

When p_e is unknown to the receiver, it can still be estimated using the *a posteriori* LLRs $L^{b_1}_{p,D_1}$ and $L^{b_2}_{p,D_2}$ of the uncoded bits b_1 and b_2 obtained by the decoders D_1 and D_2, respectively, as

$$\hat{p}_e = \frac{1}{N}\sum_{n=1}^{N} \frac{e^{L^u_{p,D_1}}+e^{L^u_{p,D2}}}{(1+e^{L^u_{p,D_1}})(1+e^{L^u_{p,D_2}})}, \quad (15)$$

where N is the number of *reliable a posteriori* LLR from both outer decoders. The LLR is reliable if the value is larger than a threshold T. The authors of [5] uses $T=3$ to estimate $\hat{p}_e$ from the extrinsic LLR. However, we found that when relatively weak code is used as in the proposed SpCC-SW system, the value should be even larger because the LLR from the weak code is unreliable, especially at low SNR range. It should be noted here that we use *a posteriori* LLR, not extrinsic LLR as in [5], to estimate p_e for more accuracy. Finally, by following (8) the correlation estimate is given by $\hat{\rho} = 1-2\hat{p}_e$.

C. Turbo FD/SC-MMSE Equalization

Since the two correlated sequences corresponding to the two sources are spatially multiplexed, a multiuser version FD/SC-MMSE presented in [15] is used. In-depth descriptions of the FD/SC-MMSE algorithm and its extension to multiuser systems are already available in many literatures, and hence, the details of turbo FD/SC-MMSE are not presented in this paper. The more detail derivation of the FD/SC-MMSE algorithm can be found, for example, in [16] and its convergence property analysis in [15].

D. Doped Accumulator

The rate-1 doped accumulator (D-ACC) [17] can be applied to fully exploit the correlation between the sources in SW systems. As shown in Fig. 2, D-ACC is performed after the interleaver. The structure of D-ACC is very simple since it is composed of a memory-1 SRCC with octal code generator of $([3,2]3)_8$ followed by heavy puncturing of the coded bits such that *coding rate* $\mathrm{R}_{dacc}=1$. With a doping rate P, the D-ACC replaces every P-th information (systematic) bits with the accumulated coded bit. At the receiver D-ACC decoding, denoted as D_{dacc}, is performed using the BCJR algorithm immediately after the equalization.[5]

[5]It should be noted here that interleaver between D_{dacc} and the equalizer is not needed because the extrinsic LLR is not iteratively exchanged between them.

III. Performances Evaluation

We conducted computer simulations to verify the effectiveness of the proposed SpCC-SW system with several values of correlation parameter ρ. Randomly generated binary sequences with length of $K = 2,560$ bits were used as b_1. The bits in b_1 was randomly flipped with probability of $p_e = \{0.00, 0.01, 0.10, 0.30, 0.49\}$.

The binary sequences b_1 and b_2 are independently coded by the same memory-3 rate $1/2$ NSNRCC encoder with generator polynomial $([17,15])_8$, resulting in two coded sequences, each having length $2K = 5,120$ coded bits. The coded sequences are further interleaved by Π_1 and Π_2 independently. The interleaver outputs are doped-accumulated with a doping rate $P=10$ and then sub-divided into 20 blocks so that each block has 256 coded bits. This number is reasonable when considering the practical fast Fourier transform (FFT) size in FD/SC-MMSE. To each of the 20 blocks, CP with 64 symbols were added, resulting in $20\times(64+256) = 6400$ BPSK symbols transmitted from each antenna, using single carrier (SC) signalling.

We assume equal average power 64-path frequency-selective block Rayleigh fading channel. The power of the symbols is normalized such that $\mathbb{E}[|s_1|^2] = \mathbb{E}[|s_2|^2] = 1$, hence $\mathbb{E}[|h_{nm}(k)|^2] = 1/(64\times 2)$, such that the receive average signal power per antenna is one, but its instantaneous power per antenna is not one. The receiver is assumed to have a perfect knowledge about the channels, but the channel is unknown to the transmitter.

In this paper, we used a notation $\alpha(\mathrm{H}\beta\mathrm{V}\eta)$ to express activation ordering patterns, where α expresses the global iteration, and β and η the *HI* and *VI* times, respectively. Similar with [13], the same pattern of $50(H1V5)$ is used throughout the paper. This pattern indicates that 1 *HI* in each branch is first performed, which is followed by 5 *VI*s; this process is repeated 50 times, which finally results in total of 2×50 *HI*s + 250 *VI*s = 350 iterations.

A. Bit-Error-Rate Performances

The average BER performance at the output of D_1 with the activation ordering pattern $50(H1V5)$ is shown in Fig. 4(a) with and without knowledge of the source correlation ρ at the receiver. The solid lines correspond to the case where ρ is known, and the dashed lines to the case where ρ is estimated using $\hat{\rho} = 1-2\hat{p}_e$. The dashed line (without marks) is the theoretical average BER of uncoded BPSK over 1-path Rayleigh fading channel for a baseline comparison indicating the upper-bound of the BER performance. Since this paper considers relatively weak codes compared with the Turbo codes in [5], the threshold T was set at 3 for $\rho = \{0.02, 0.4, 0.8\}$ and 6 for $\rho = \{0.98, 1.00\}$ to select only the reliable *a posteriori* LLRs from D_1 and D_2. It is found that with the threshold setting described above, the BER performance with estimated $\hat{\rho}$ is almost the same as the BER performance with known ρ.

We also evaluate for comparison the BER performance of SuTC presented in [5] over the same channel model using exactly the same FD/SC-MMSE turbo equlization. SuTC has internal loop (*IL*) inside the Turbo decoder and external loop (*EL*) between the Turbo decoders. Only one *IL* was performed for the decoding of each Turbo code, as in [5].

For fair comparison, we performed SuTC decoding with activation ordering pattern $50(H1I1E4)$ which results in $2\times 50\ HIs + 2\times 50IL + 200\times ELs$ = 400 iterations, and hence the total activation times with SpCC-SW is still lower. Furthermore, it should be emphasized that the complexity required for the decoders are significantly different: SuTC has 4 memory-3 convolutional codes, while the proposed SpCC-SW system has only 2 memory-3 convolutional codes and 2 memory-1 doped accumulators.

Since [5] assumes symmetric design $R_{C_1} = R_{C_2} = 1/2$, convolutional constituent code output is punctured for the rate adjustment with the puncturing pattern $Punct_1 = Punct_2 = [1\ 1; 1\ 0; 0\ 1]$ [18], which is common to the two Turbo encoders. The other puncturing patterns, e.g., in [18] may be used, however, since the difference is minor, and furthermore, since this paper's aims is not on the code optimization, we used the puncturing pattern $Punct_1 = Punct_2 = [1\ 1; 1\ 0; 0\ 1]$. The BER performance of SuTC is shown in Fig. 4(b) where clear turbo cliff happens only when $\rho = 1.0$.

The BER curves shown in Fig. 4 are for $\rho = \{1.00, 0.98, 0.80, 0.40, 0.02\}$. The figure indicates that the proposed SpCC-SW significantly outperforms SuTC for all possible correlations. Furthermore, with SuTC the BER curves exhibit error floors when $\rho < 1.00$, while with SpCC-SW, the BER curves have no error floors in the range of average BER shown in the figure as expected from the EXIT analysis in the next section.

B. EXIT Analysis

Fig. 3 shows the EXIT curves of $EQ+D_{dacc}$ for a single snapshot of channel realizations at SNR $= -5$ dB and the EXIT curves of the joint decoders for $\rho = \{0.0, 0.8, 0.98, 1.0\}$. The trajectory is shown only for $\rho = 1.0$.[6] $I^{x'}_{a_1,EQ} = I(L^{x'}_{a_1,EQ}; x')$ and $I^{y'}_{a_2,EQ} = I(L^{y'}_{a_2,EQ}; y')$ denote *a priori* mutual informations (MI) between the *a priori* LLR $L^{x'}_{a_1,EQ}$ for antenna 1 and bit x', and between *a priori* LLR $L^{y'}_{a_2,EQ}$ for antenna 2 and bit y', respectively [19]. Similarly, the MI for extrinsic LLR at antennas 1 and 2 are denoted by $I^{x'}_{e_1,EQ}$ and $I^{y'}_{e_2,EQ}$, respectively.

It is found from Fig. 3 that the convergence tunnel opens until a point very close to the (1.0,1.0) MI point, resulting in the lowering error floor[7] as well as better matching with the EQ+D_{dacc} and decoders' EXIT curves. Fig. 3 also shows that, with 5 *VI*s the EXIT curves of the decoders are pushed down as the correlation ρ increases, which makes the convergence tunnel opens even at lower SNRs. It is also indicated in the figure that the doping rate of neither $P = 1$ (full accumulator) nor $P = 100$ is a suitable choice, since the EXIT curves intersect at points "A" and "B" as shown in Fig. 3, respectively. Based on this observation, we set the doping rate at $P = 10$ throughout the paper for better matching of the curves for all the correlation values ρ considered.

C. Analysis on Slepian-Wolf Region at 1% Outage Probability

We consider the MIMO channel capacity, as in [20], because the proposed SpCC-SW has two receive antennas and each of the two users has one antenna, which can be viewed as a virtual 2×2 MIMO channel. The Slepian-Wolf and Shannon theorems states that the condition for achieving arbitrarily low BER for two correlated sources, b_1 and b_2, is

$$\mathcal{H}(b_1, b_2) \leq \mathcal{C}_{\text{MIMO}}(\Gamma), \tag{16}$$

where $\mathcal{C}_{\text{MIMO}}(\Gamma)$ denotes the MIMO channel capacity and the condition is "if and only if". The SW-Shannon limit for MIMO channel, Γ^{mimo}_{lim}, is obtained by setting $\mathcal{C}_{\text{MIMO}}(\Gamma) = \mathcal{R}_{SW}$.

However, in fading channels, the capacity itself is a random variable. Therefore, when considering how close the performance of our proposed SpCC-SW system is to the SW-Shannon limit, we need to evaluate the outage capacity. For this purpose, we evaluated the complementary cumulative distribution function (CCDF) of the MIMO capacity from many channel realizations characterized by the equal average power 64-path frequency-selective block Rayleigh fading channels. We consider 1% outage capacity, $\mathcal{C}^{99\%}_{\text{MIMO}}$, yielding

$$\Pr(\mathcal{C}^{99\%}_{\text{MIMO}}) \leq \mathcal{H}(b_1, b_2) = 0.01. \tag{17}$$

The CCDF curve shown in Fig. 5 were obtained by the two methods. One is by first pre-setting Γ and generating many channel realizations, all having the pre-set Γ, and obtain the CCDF of $\mathcal{C}^{99\%}_{\text{MIMO}} = \mathcal{R}_{SW}$. If the $\mathcal{C}^{99\%}_{\text{MIMO}}$ is lower/higher than the $\mathcal{R}_{SW}$, increase/decrease gradually the pre-set Γ. When the Γ yielding $\mathcal{C}^{99\%}_{\text{MIMO}} = \mathcal{R}_{SW}$, the simulation was stopped and the value Γ was used as the SW/Shannon limit, denoted as Γ_{lim}. Another method was to find the outage capacity based on the value Γ in Fig. 4 that achieve BER $= 10^{-5}$. The CCDF obtained by the first method is shown by the solid curve and the second method is by the dashed curve, both in Fig. 5. Table I shows the performance comparison between the proposed SpCC-SW and the SuTC techniques and their gaps in dB to the theoretical limit Γ_{lim} value obtained by the techniques described above. From Fig. 4 and Table I, it can be observed that our proposed SpCC-SW technique outperforms SuTC, with the gap to the SW/Shannon limit is 1.02-1.28 dB for all ρ values tested, while the gap with SuTC is 3.15-5.90 dB to the limit.

TABLE I
SYSTEM PERFORMANCES OF SUTC AND OUR PROPOSED SPCC-SW AT BER = 10^{-5}

p_e	$\mathcal{H}(b_1,b_2)$	$\mathcal{R}_{\text{SW}}$	Γ_{lim} (Theory)	SuTC [dB] (Simulation)		Proposed [dB] (Simulation)	
				Γ	Gap	Γ	Gap
0.00	1.000	0.250	–5.40	–2.25	3.15	–4.38	1.02
0.01	1.081	0.270	–5.05	0.25	5.30	–3.88	1.17
0.10	1.469	0.367	–3.15	3.25	6.40	–1.88	1.27
0.30	1.881	0.470	–1.50	4.75	6.25	–0.25	1.25
0.49	1.999	0.499	–1.15	4.75	5.90	0.13	1.28

The SW region obtained by (12) and the rate region with $\mathcal{C}^{99\%}_{\text{MIMO}} = \mathcal{R}_{SW}$ are plotted in Fig. 6, both by solid lines. The rates obtained from the proposed SpCC-SW is plotted by "•" for the correlation parameters (i) $\rho = 1.00$, (ii) $\rho = 0.98$, (iii) $\rho = 0.40$, and (iv) $\rho = 0.02$. It is found that with 99% of probability, the mark "•" is within the SW region, and furthermore the SW region and the rate region obtained from the second method have intersection at a point that divides equally the rate to the two sources.[8] This assures that the source and channel separation holds with 99% of probability with our proposed SpCC-SW system. In fact, theoretical analyses presented in this paper do not assume that the channel coding is designed by taking into account the source correlation property. This is consistent to the observation described above.

IV. CONCLUSION

In this paper, a simple coding structure for Slepian-Wolf system over multipath-rich frequency-selective block Rayleigh fading channels is proposed for two correlated sources, where the correlation is expressed by the bit-flipping model. The proposed SpCC-SW system has two types of turbo loops, *HI* and *VI*, to achieve diversity and coding gains and utilized a rate-1 D-ACC to flexibly adapt the variation of the correlation between the sources. The results confirm that in multipath-rich environments the proposed structure, even with relatively weak channel codes, can achieve very excellent performance, 1.02–1.28 dB away from the SW-Shannon limit, at all values of the source correlation. EXIT chart shows that the proposed

[6] For the shake of simplicity and clear visibility of the figure.

[7] The floor is unobserved until a BER of 10^{-5}, as shown in Fig. 4(a).

[8] It should be noted here that the BER performance shown in Fig. 4 are the same for each source.

SpCC-SW structure has better matching EXIT curves, which provide near-Shannon-SW limit performance. Results of analysis on MAC and SW regions have found that with the proposed SpCC-SW system the rate region obtained by the massive simulations conducted at 1% outage capacity and the theoretical SW region have *intersection* with 99% probability, and hence *the source channel separation holds* with the probability.

REFERENCES

[1] J. Chou, D. Petrovic, and K. Ramchandran, "A distributed and adaptive signal processing approach to reducing energy consumption in sensor networks," in *IEEE INFOCOM*, Sept. 2004.

[2] C. Douillard, C. M. Jezequel, C. Berrou, A. Picart, P. Didier, and A. Glavieux, "Iterative correction of intersymbol interference: Turbo-equalization," *Eur. Trans. Telecommun.*, vol. 6, no. 5, pp. 507–511, Sept. 1995.

[3] J. D. Ser, P. Crespo, and A. Munoz, "Joint source-channel decoding of correlated sources over ISI channels," in *IEEE VTC-Spring*, Los Alamitos, May 2005.

[4] J. D. Ser, P. M. Crespo, C. J. Mitchell, and M. Fauri, "Iterative equalization and decoding of correlated sources over the frequency vector gaussian multiaccess channel," in *Workshop on Smart Antennas-WSA*, Ulm (Alemania), March 2006.

[5] J. Garcia-Frias and Y. Zhao, "Near-Shannon/Slepian-wolf performance for unknown correlated sources over AWGN channels," *IEEE Trans. on Comm.*, vol. 53, no. 4, pp. 555–559, April 2005.

[6] Y. Zhao, W. Zhing, and J. Garcia-Frias, "Transmission of correlated senders over a rayleigh fading multiple access channel," *Elsevier Signal Processing*, vol. 86, pp. 3150–3159, April 2006.

[7] D. Slepian and J. K. Wolf, "Noiseless coding of correlated information sources," *IEEE Trans. on Information Theory*, vol. 19, pp. 471–480, July 1973.

[8] Z. Xiong, A. D. Liveris, and S. Cheng, "Distributed source coding for sensor networks," *IEEE Signal Processing Magazine*, pp. 80–94, Sept. 2004.

[9] R. Puri and K. Ramchandran, "PRISM: A new robust video coding architecture based on distributed compression principles," in *Allerton Conf. on Comm, Control, and Computing*, Allerton, IL, Oct. 2002.

[10] M. Johnson, P. Ishwar, V. M. Prabhakaran, D. Schonberg, and K. Ramchandran, "On compressing encrypted data," *IEEE Trans. on Signal Processing*, no. 10, pp. 2992–3006, Oct. 2004.

[11] R. Cristescu, B. Beferull-Lozano, and M. Vetterli, "Networked Slepian-Wolf: Theory, algorithm and scaling laws," *IEEE Trans. on Information Theory*, vol. 51, no. 12, pp. 4057–4073, Dec. 2005.

[12] T. Abe, S. Tomisato, and T. Matsumoto, "A MIMO turbo equalizer for frequency-selective channels with unknown interference," *IEEE Trans. on Vehicular Technology*, vol. 52, no. 3, pp. 476–482, May 2003.

[13] K. Anwar and T. Matsumoto, "MIMO spatial turbo coding with iterative equalization," in *ITG Workshop on Smart Antennas*, Bremen, Germany, Feb. 2010.

[14] L. Bahl, J. Cocke, F. Jelinek, and J. Raviv, "Optimal decoding of linear codes for minimizing symbol error rate," *IEEE Trans. on Info. Theory*, vol. IT-20(2), pp. 284–287, March 1974.

[15] K. Kansanen and T. Matsumoto, "An analitical method for MMSE MIMO turbo equalizer EXIT chart computation," *IEEE Trans. Wireless Comm.*, vol. 6, no. 1, pp. 59–63, Jan. 2007.

[16] M. Tuchler, R. Koetter, and A. Singer, "Turbo equalization: Principles and new results," *IEEE Trans. on Comm.*, vol. 50, no. 5, pp. 754–767, May 2002.

[17] S. Pfletschinger and F. Sanzi, "Error floor removal for bit-interleaved coded modulation with iterative detection," *IEEE Trans. on Wireless Communications*, vol. 5, no. 11, pp. 3174–3181, Nov. 2006.

[18] I. Land and P. Hoeher, "Partially systematic rate 1/2 turbo codes," in *Int. Symp. Turbo Codes*, Brest, France, Sept. 2000.

[19] S. ten Brink, "Convergence behavior of iteratively decoded parallel concatenated codes," *IEEE Trans. Commun.*, vol. 49, pp. 1727–1737, Oct. 2001.

[20] C. B. Schlegel and L. C. Perez, *Trellis and Turbo Coding*. IEEE Press and Wiley Inter-science, 2004.

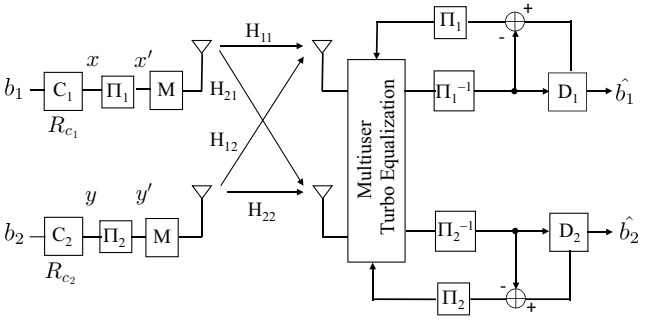

Fig. 1. Multi-user communication as special case of uncorrelated sources system

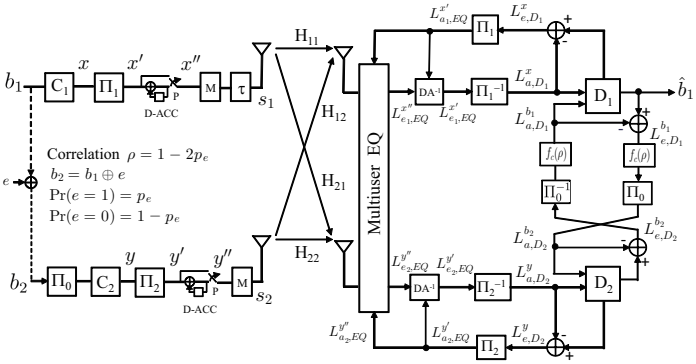

Fig. 2. Proposed SpCC-SW for Slepian-Wolf coding systems with D-ACC. A delay of τ is added to compensate the additional interleaver Π_0 between the sources b_1 and b_2.

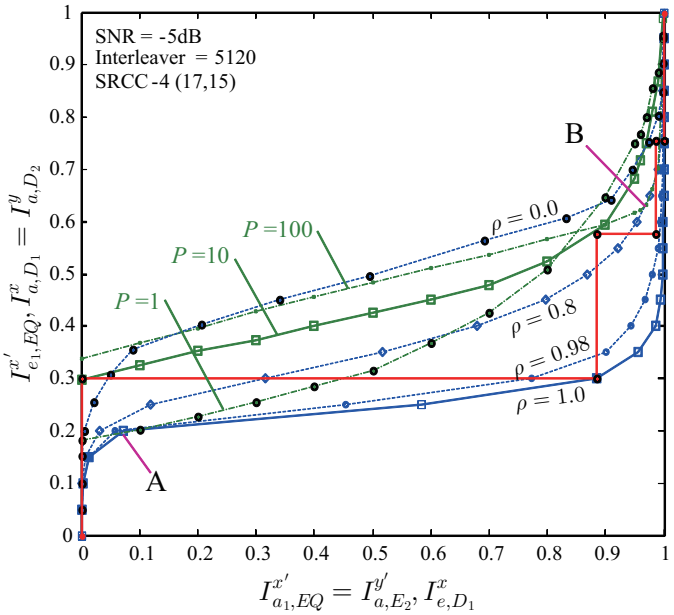

Fig. 3. EXIT chart of FD/SC-MMSE Equalizer + D-ACC at SNR $= -5$ dB and joint decoders with $\rho = \{0.0, 0.8, 0.98, 1.0\}$ and its corresponding trajectory for $\rho = 1.0$

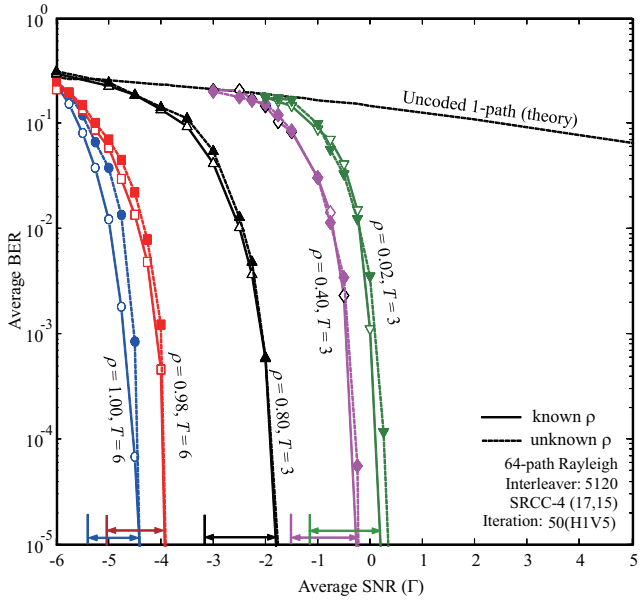

(a) The proposed SpCC-SW

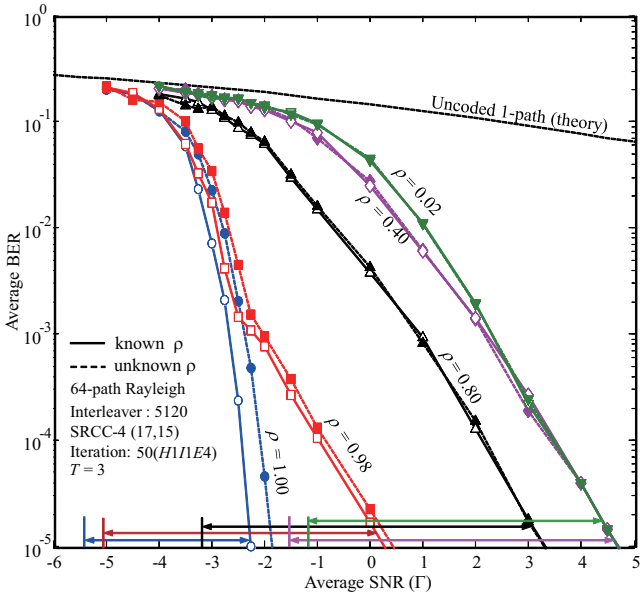

(b) SuTC in [5]

Fig. 4. BER Performances vs. average SNR (Γ) of SpCC-SW and SuTC systems over MIMO channel with 64-path equal average power Rayleigh fading channel and their capacity limits

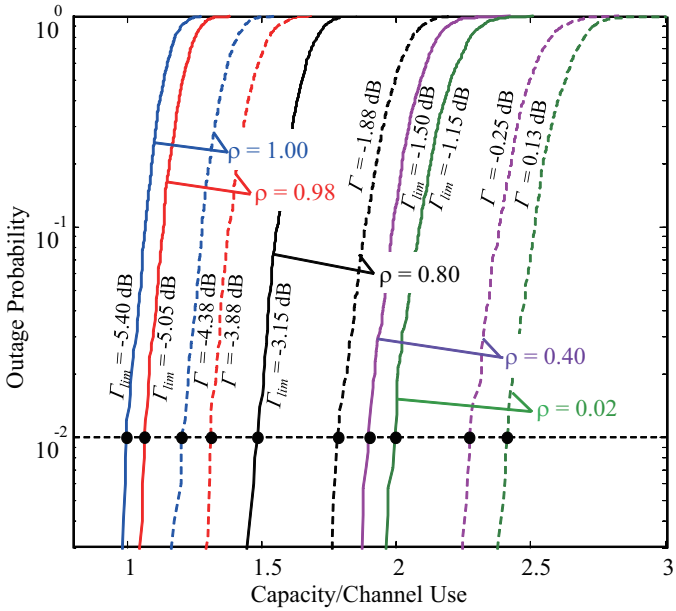

Fig. 5. CCDF of the theoretical and experimental MIMO capacities (Note: Γ is Γ at BER= 10^{-5})

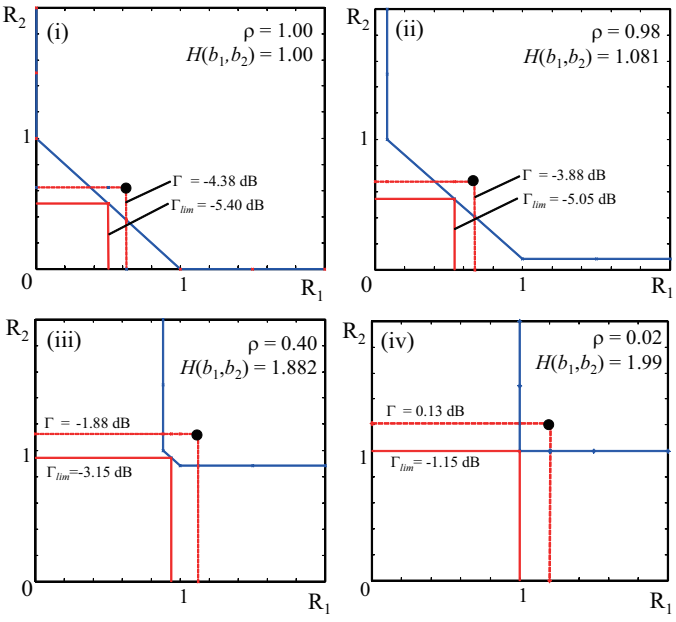

Fig. 6. Theoretical rate regions and experimental 99% MAC regions: (i) $\rho = 1.00$, (ii) $\rho = 0.98$, (iii) $\rho = 0.40$ and (iv) $\rho = 0.02$ (Note: Γ is Γ at BER= 10^{-5})